

W/Z Production : Asymmetry, Z(p_T), and W+charm at the Tevatron

Jiyeon Han for the CDF and DØ Collaborations
*Department of Physics and Astronomy, University of Rochester,
Rochester NY 14627-0171, USA*



We report on W/Z production processes at the Tevatron, including the W charge asymmetry, the Z boson rapidity and p_T distributions, and the W+charm final state. The measurements test the Standard Model and yield constraints on parton distribution functions. The data samples used range from 0.3 to 2.1 fb^{-1} of $p\bar{p}$ collisions at $\sqrt{s}=1.96$ TeV.

1 W/Z production at the Tevatron

1.1 Electroweak Physics at Tevatron

Investigations of electroweak processes at the Tevatron have focussed on three different areas: (a) the W mass and width, (b) diboson production, and (c) details of W/Z production processes. Precise measurements of the W mass constrain the mass of the Higgs boson, and measurements of the W width can be compared with Standard Model (SM) predictions. Diboson production provides information on gauge boson self-interactions and is sensitive to physics beyond the SM. Understanding diboson production is also relevant to new particle searches because it is the background to Higgs and SUSY particle production. Measurement of details of W/Z production processes, such Z boson rapidity and p_T distributions and the W charge asymmetry provide information on the up and down parton distribution functions (PDFs) in the proton, while the W+charm cross section is sensitive to the PDF of strange quarks.

1.2 Detectors

We report on results from CDF and DØ Tevatron experiments at Fermilab. The CDF detector has a larger tracking volume which yields better momentum resolution for charged tracks than the DØ detector in the central region. The DØ detector has a larger muon acceptance and more coverage in the forward rapidity region.^{1,2}

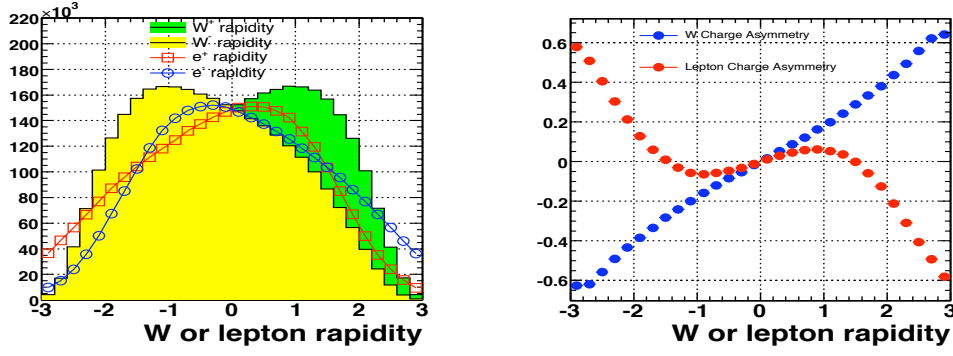


Figure 1: The left figure shows the W boson and lepton rapidity distribution. The right figure replaces the plot with the predicted W and lepton charge asymmetries.

1.3 W Boson and Lepton Charge Asymmetry

$W^+(W^-)$ events are produced in the collisions of $u(\bar{u})$ and $\bar{d}(d)$ quarks. Since, on average, the $u(\bar{u})$ quark carries a higher momentum fraction than the $\bar{d}(d)$ quark, the $W^+(W^-)$ is boosted along the proton (anti-proton) direction. This results in a W charge asymmetry. The W charge asymmetry ($A(y_W)$) is defined as :

$$A(y_W) = \frac{d\sigma(W^+)/dy_W - d\sigma(W^-)/dy_W}{d\sigma(W^+)/dy_W + d\sigma(W^-)/dy_W} \quad (1)$$

At LO, it can be described in terms of the momentum fractions of the u and d quarks :

$$A(y_W) \approx \frac{d(x_2)/u(x_2) - d(x_1)/u(x_1)}{d(x_2)/u(x_2) + d(x_1)/u(x_1)} \quad (2)$$

where $x_{1,2} = \frac{M_W}{\sqrt{s}} e^{\pm y_W}$. The $A(y_W)$ is sensitive to slope of $d(x)/u(x)$.

Experimentally, the lepton charge asymmetry is measured:

$$A(\eta_\ell) = \frac{d\sigma(\ell^+)/d\eta_\ell - d\sigma(\ell^-)/d\eta_\ell}{d\sigma(\ell^+)/d\eta_\ell + d\sigma(\ell^-)/d\eta_\ell} \quad (3)$$

The measured lepton charge asymmetry is a convolution of the W charge asymmetry, and the asymmetry from the V-A interaction. Figure 1 shows the W boson and the lepton rapidity distributions and the resulting W and lepton charge asymmetries.

At large lepton pseudorapidities, the V-A interaction distorts the boson production asymmetry.

DØ and CDF collaboration use different approaches in the measurement of the W asymmetry. The DØ collaboration uses the traditional method of measuring the charge asymmetry in the muon decay channel. The data sample consists of 0.3 fb^{-1} . Figure 2 shows the lepton charge asymmetry versus muon pseudorapidity. The central region measurements by both CDF and DØ ($|\eta_\mu| < 1.3$) have been used to constrain PDFs in previous fits. The high rapidity region ($|\eta_\mu| > 1.3$) probes the PDFs at higher x. The high rapidity region is still statistics limited.

A new measurement by the CDF collaboration extracts the W charge asymmetry from the lepton charge asymmetry. The W boson rapidity (y_W) can be determined from the 4-momentum of the final state neutrino. However, the momentum of the neutrino in z-direction (P_z^ν) is not measured and only its transverse momentum is known (the missing transverse energy of the event). The P_z^ν is calculated as follows:

$$M_W^2 = (E_\ell + E_\nu)^2 - (P_\ell + P_\nu)^2 \quad (4)$$

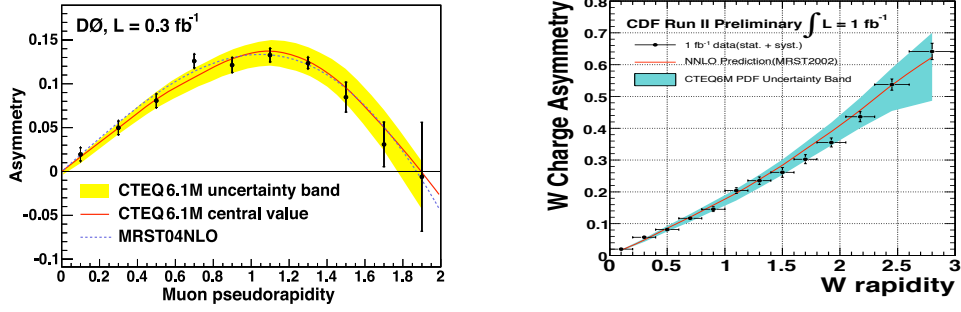


Figure 2: The left plot shows the lepton charge asymmetry in muon pseudorapidity measured in $D\emptyset$, and the right plot shows the W boson charge asymmetry in boson rapidity measured in CDF.

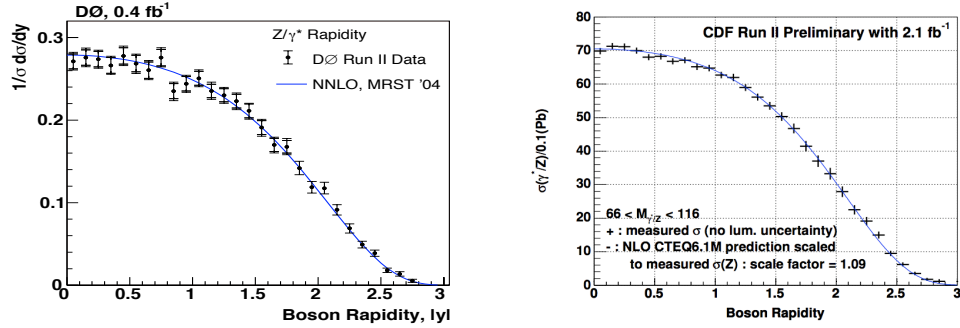


Figure 3: Z boson rapidity distributions. The left plot is the normalized of Z boson rapidity distribution measured at $D\emptyset$, and the right plot is the Z boson rapidity measured at CDF. The theory prediction is normalized to the measured total σ .

where M_W is constrained to the W boson mass. There are two solutions for P_z^ν . Each P_z^ν solution is weighted by a factor which includes the W^\pm production cross section ($d\sigma/dy_W$), the V-A angular distribution function in the center-of-mass frame ($1 \pm \cos^2\theta^*$), and a W^\pm transverse momentum (P_T^W) factor to account for higher order QCD corrections to the V-A $\cos\theta^*$ term. The dependence on input $d\sigma/dy_W$ is removed by iterating the measurement. Each iteration is used further to constrain $d\sigma/dy_W$. Here, the larger acceptance electron sample with 1 fb^{-1} is used.

The W charge asymmetry for 1 fb^{-1} data is shown in Figure 2. There is good agreement with the NNLO prediction using MRST2002 PDFs.^{5,6} The experimental error is smaller than the current uncertainty in the PDFs, and the new data can be used further constrain PDFs in future fits.

1.4 The Z Boson Rapidity Distribution: $d\sigma/dy$

In the Drell-Yan process, the quark and anti-quark carry parton momentum fractions, x_1 and x_2 . The difference in the parton momentum fractions ($x_{1,2}$) determine the rapidity of the final state Z boson (y_Z). Since high y_Z corresponds to high x_1 and low x_2 , this region probes PDFs at high x. In addition, the $d\sigma/dy$ distribution tests QCD theory predictions at higher orders. In higher order (NLO or NNLO), gluons splitting in the initial state also contribute to the rapidity distribution. Both $D\emptyset$ and CDF measure $d\sigma/dy$ using the dielectron final state. In both measurements, y_Z measurements extend up to 2.9. The $D\emptyset$ measurement, shown in Figure 3, with 0.4 fb^{-1} shows good agreement with the NNLO MRST⁷ prediction. The CDF measurement, also shown in Figure 3, uses 2.1 fb^{-1} . Figure 4 shows the ratio of the CDF data to the NLO calculation with NLO CTEQ6.1M PDFs.⁸

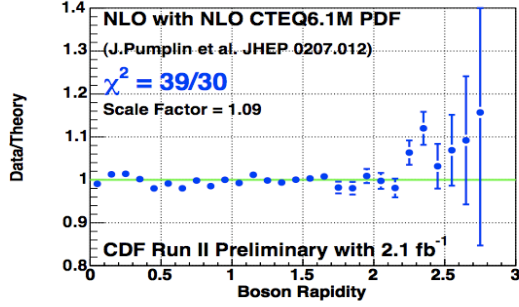


Figure 4: Ratio of data and theory prediction for the Z boson rapidity distribution in CDF. Here, the NLO calculation with NLO CTEQ6.1M PDFs is used. The theory prediction is normalized to the measured σ .

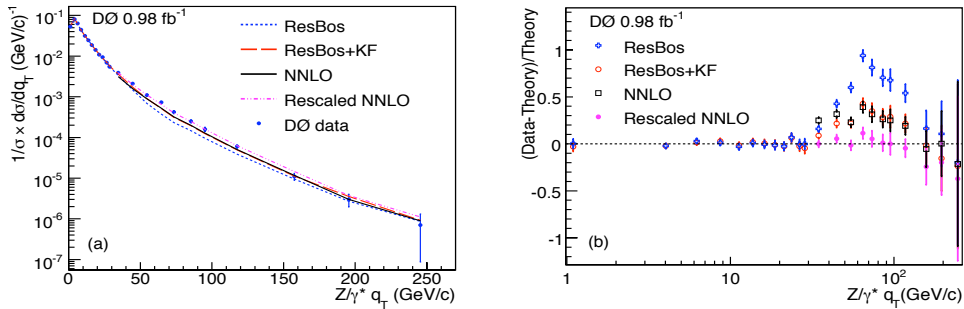


Figure 5: The left plot shows the normalized differential cross section of Z boson p_T up to $p_T < 260 \text{ GeV}/c$. The right plot shows the fractional difference between data and the theory predictions. “KF” is the scale factor(K-factor) of NLO to NNLO theory calculation.

1.5 $Z(p_T)$ Distribution

The Z boson p_T which can be measured over a wide range of values provide a test of QCD. In the $p_T > 30 \text{ GeV}/c$ region, where the p_T originates from the radiation of energetic gluons, the perturbative QCD calculation⁹(NNLO¹⁰) gives reliable predictions. In the $p_T < 30 \text{ GeV}/c$ region, where multiple soft gluon emission is dominant, the soft gluon resummation technique is used (ResBos).^{11,12} The $D\theta$ measurement in the Z with 0.98 fb^{-1} of data in the ee channel is shown in Figure 5. The ResBos curve is the gluon resummation calculation including PHOTOS¹⁵, which accounts for radiated photons in the final state. The “Rescaled NNLO” is the NNLO calculation rescaled to match the data at $p_T = 30 \text{ GeV}/c$. The right hand side of Figure 5 shows the fractional differences between the data and theory on a linear scale. In the $p_T < 30 \text{ GeV}/c$ region, the ResBos calculation describes the data well. For $p_T > 30 \text{ GeV}/c$, the data is higher than all predictions. The NNLO theory prediction agrees with the data only in shape.

$D\theta$ also investigated the “Small-x broadening effect”^{13,14} that predicts a wider p_T distribution in the large rapidity region. This effect modifies the resummation form factor in the small-x parton region. At the Tevatron, Z bosons with $2 < |y| < 3$ probe the Bjorken x region, $0.002 < |x| < 0.006$. Therefore, a measurement of the Z boson p_T in the high rapidity region is sensitive to the modified form factor. Figure 6 shows the $p_T < 30 \text{ GeV}/c$ region for all y_Z and for $|y_Z| > 2$. The standard ResBos calculation agrees well with the data in all y_Z . The $|y_Z| > 2$ region data does not favor an additional small-x form factor. This is the first test of the “small-x broadening effect” using the high y region at the Tevatron.

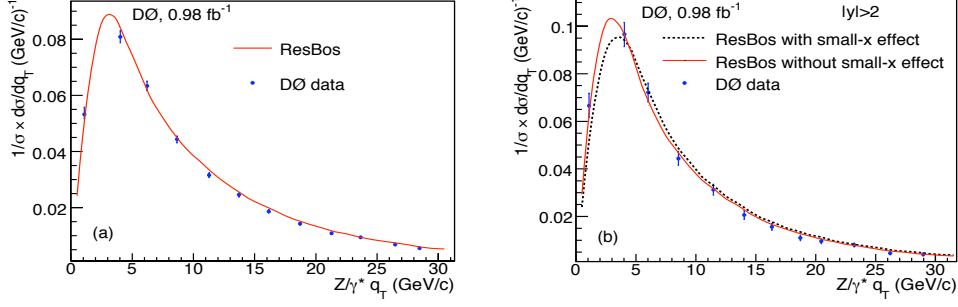


Figure 6: The plots show the normalized differential cross section of Z boson p_T measured at DØ. The left plot shows the result for all boson rapidity, and the right plot shows the result in the high rapidity region ($|y_Z| > 2$), which is sensitive to the “small-x broadening effect”.

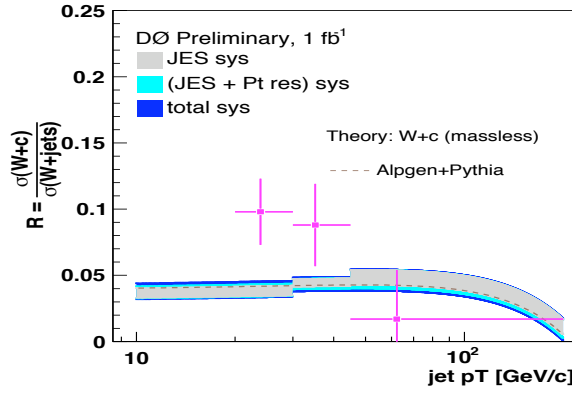


Figure 7: The cross section ratio W+c-jet to W+jets measured at DØ.

1.6 W+Charm Cross Section

The W+charm process, $g + s \rightarrow W^- + c$, is a background to top, SUSY particle, and SM Higgs production. Since CKM matrix element, $|V_{cd}|^2$ suppresses the d-quark-gluon fusion production, the W+charm production probes the s-quark PDF. Strange quarks contributes to the processes, $p\bar{p}/pp \rightarrow sg \rightarrow W^- + c$ and $p\bar{p}/pp \rightarrow s\bar{c} \rightarrow H^-$, at the Tevatron and LHC. At hadron colliders, the s-quark distribution is probed at large $Q^2 \approx M_W^2$.

The DØ and CDF collaborations tag the c-jet by looking for the muon from the decay of the charm particle in the c-jet. The muon from the decay of the charm particle and the lepton from the W boson decay have the opposite electric charge. The opposite charge requirement is used in the event selection. All leptonic channels are allowed for the W boson decay. $Z \rightarrow \mu\mu$ events are rejected by requiring $M_{\mu\mu} < 70 \text{ GeV}/c^2$ for the muon decay channel. DØ measures the cross section ratio of the W+c-jet to W+jets processes, $\frac{\sigma(p\bar{p} \rightarrow W+c-jet)}{\sigma(p\bar{p} \rightarrow W+jets)}$, using 1 fb^{-1} data. The fraction of $\sigma(W + c - jet)$ compared with the theory versus jet p_T is shown in Figure 7. The fraction of $\sigma(W + c - jet)$ for $p_T > 20 \text{ GeV}/c$ is 0.071 ± 0.017 . The measured fraction in the electron channel is $0.060 \pm 0.021(stat.)_{-0.007}^{+0.005}(sys.)$ and the fraction in the muon channel is $0.093 \pm 0.029(stat.) \pm 0.005(sys.)$.

CDF measures the total cross section of W+c-jet with 1.8 fb^{-1} data. Both electron and muon channels are used for the W boson selection. The c-jets with $p_T(c) > 20 \text{ GeV}/c$ and $|\eta(c)| < 1.5$ are identified using the semi-muonic decay of the charm particle in the jet. The measured cross section for the leptonic channel, $\sigma_{Wc} \times BR(W \rightarrow \ell\nu)$, is $9.8 \pm 2.8(stat.)_{-1.6}^{+1.4}(sys.) \pm 0.6(lum) \text{ pb}$,

which agrees with the NLO calculation, $11.0_{-3.0}^{+1.4}pb$.

1.7 Conclusion

New high statistics measurements of W and Z production processes at the Tevatron are used to provide new constraints on nucleon PDFs. The W charge asymmetry and Z boson $d\sigma/dy$ measurement have been extended up to $y \approx 2.9$. The Z boson $d\sigma/dy$ measurement is with 2.1 fb^{-1} of data, and 8 fb^{-1} is expected by end of 2009.

Acknowledgments

We thank the CDF and D0 collaborations, the Fermilab staff, and the members of the University of Rochester CDF group.

References

1. D. Acosta et al. (CDF Collaboration) , *Phys. Rev. D* **71**, 052003 (2005).
2. B. Abbott et al. (D0 Collaboration) , *Phys. Rev. D* **61**, 032004 (2000).
3. J. Pumpkin et al. , *JHEP* **0207**, 012 (2002) and D. Stump et al. , *JHEP* **0310**, 046 (2003).
4. A.D. Martin et al. (MRST Collaboration), *Phys. Lett. B* **604**, 61 (2004).
5. C. Anastasiou et al. , *Phys. Rev. D* **D69**, 094008 (2004).
6. A.D. Martin, R.G. Roberts, W.J. Stirling and R.S. Thorne (MRST Collaboration), *EPJ* **C28**, 455 (2003).
7. L. Dixon et al. (MRST Collaboration) , *Phys. Rev. D* **69**, 09408 (2004).
8. J. Pumplin et al. (CTEQ Collaboration), hep-ph/ **0201195**, 455 (2002).
9. P.B. Arnold and M.H. Reno , *Nucl. Phys.* **B319**, 37 (1989); R.J. Gonsalves, J. Pawlowski and C-F. Wai , *Phys. Rev. D* **40**, 2245 (1989);.
10. K. Melnikov and F. Petriello , *Phys. Rev. D* **74**, 114017 (2006).
11. C. Balazs and C.P Yuan , *Phys. Rev. D* **56**, 5558 (1997)
12. P.B. Arnold and R. Kauffman , *Nucl. Phys.* **B349**, 381 (1991).
13. P. Nadolsky, D.R. Stump, and C.P. Yuan , *Phys. Rev. D* **61**, 014003 (2000).
14. P. Nadolsky, D.R. Stump, and C.P. Yuan , *Phys. Rev. D* **64**, 114011 (2001).
15. E. Barberio and Z. Was , *Comput. Phys. Commun.* **79**, 291 (1994).